NASA/TM-2001-211253

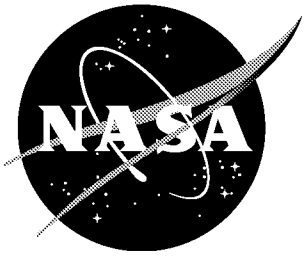

Hypersonic Flows About a 25° Sharp Cone

James N. Moss
Langley Research Center, Hampton, Virginia

December 2001

The NASA STI Program Office ... in Profile

Since its founding, NASA has been dedicated to the advancement of aeronautics and space science. The NASA Scientific and Technical Information (STI) Program Office plays a key part in helping NASA maintain this important role.

The NASA STI Program Office is operated by Langley Research Center, the lead center for NASA's scientific and technical information. The NASA STI Program Office provides access to the NASA STI Database, the largest collection of aeronautical and space science STI in the world. The Program Office is also NASA's institutional mechanism for disseminating the results of its research and development activities. These results are published by NASA in the NASA STI Report Series, which includes the following report types:

- TECHNICAL PUBLICATION. Reports of completed research or a major significant phase of research that present the results of NASA programs and include extensive data or theoretical analysis. Includes compilations of significant scientific and technical data and information deemed to be of continuing reference value. NASA counterpart of peer-reviewed formal professional papers, but having less stringent limitations on manuscript length and extent of graphic presentations.

- TECHNICAL MEMORANDUM. Scientific and technical findings that are preliminary or of specialized interest, e.g., quick release reports, working papers, and bibliographies that contain minimal annotation. Does not contain extensive analysis.

- CONTRACTOR REPORT. Scientific and technical findings by NASA-sponsored contractors and grantees.

- CONFERENCE PUBLICATION. Collected papers from scientific and technical conferences, symposia, seminars, or other meetings sponsored or co-sponsored by NASA.

- SPECIAL PUBLICATION. Scientific, technical, or historical information from NASA programs, projects, and missions, often concerned with subjects having substantial public interest.

- TECHNICAL TRANSLATION. English-language translations of foreign scientific and technical material pertinent to NASA's mission.

Specialized services that complement the STI Program Office's diverse offerings include creating custom thesauri, building customized databases, organizing and publishing research results ... even providing videos.

For more information about the NASA STI Program Office, see the following:

- Access the NASA STI Program Home Page at ***http://www.sti.nasa.gov***

- E-mail your question via the Internet to help@sti.nasa.gov

- Fax your question to the NASA STI Help Desk at (301) 621-0134

- Phone the NASA STI Help Desk at (301) 621-0390

- Write to:
  NASA STI Help Desk
  NASA Center for AeroSpace Information
  7121 Standard Drive
  Hanover, MD 21076-1320

NASA/TM-2001-211253

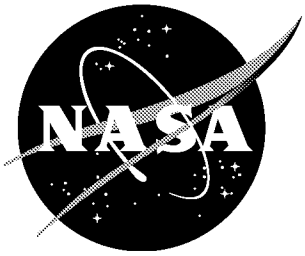

Hypersonic Flows About a 25° Sharp Cone

James N. Moss
Langley Research Center, Hampton, Virginia

National Aeronautics and
Space Administration

Langley Research Center
Hampton, Virginia 23681-2199

December 2001

Available from:

NASA Center for AeroSpace Information (CASI)
7121 Standard Drive
Hanover, MD 21076-1320
(301) 621-0390

National Technical Information Service (NTIS)
5285 Port Royal Road
Springfield, VA 22161-2171
(703) 605-6000

Hypersonic Flows About a 25° Sharp Cone

James N. Moss

NASA Langley Research Center, MS 408A, Hampton, VA 23681-2199

Abstract. This paper presents the results of a numerical study that examines the surface heating discrepancies observed between computed and measured values along a sharp cone. With Mach numbers of an order of 10 and the free-stream length Reynolds number of an order of 10 000, the present computations have been made with the direct simulation Monte Carlo (DSMC) method by using the G2 code of Bird. The flow conditions are those specified for two experiments conducted in the Veridian 48-inch Hypersonic Shock Tunnel. Axisymmetric simulations are made since the test model was assumed to be at zero incidence. Details of the current calculations are presented, along with comparisons between the experimental data, for surface heating and pressure distributions. Results of the comparisons show major differences in measured and calculated results for heating distributions, with differences in excess of 25 percent for the two cases examined.

INTRODUCTION

Recent experiments [1] conducted in hypersonic impulse facilities by Calspan University of Buffalo Research Center (CUBRC) personnel provide a substantial experimental database for hypersonic flows about hollow cylinder-flare and double cone models. These tests were conducted in nitrogen and included surface measurements for heating and pressure and for schlieren imagery at Mach numbers ranging from 9.3 to 11.5. Computations, using both computational fluid dynamics (CFD) and DSMC methods, have been performed for several of the CUBRC experiments, and an initial comparison and assessment of the experimental and computational data was presented in Ref. [2] (details concerning the computations are given in Refs. [3] to [8]). Closer examination of the experimental/computational results showed significant differences between most of the computed and measured heating rates, even upstream of the complex interactions induced by the compression surfaces. With the exception of the results obtained with a DSMC code called MONACO [7], the CFD and DSMC simulations have predominately produced heating rate values that are high in relation to the measured values. (**Note that a recent determination has been made that the MONACO results cited herein are in error, as explained in the Concluding Remarks section.**) The same trends are evident in the calculations (see Refs. [9] to [11]) that have been presented after the release of the experimental results. Currently, the source of the discrepancies has not been identified; however, additional experiments are scheduled by CUBRC to help clarify this issue.

With an ongoing reconciliation process evolving for the CUBRC test cases, computational studies [10] have begun to focus on the sharp cone portion of the double cone model; that is, that portion of the model not affected by the presence of the second cone. Such is the focus of the current study in which calculations for a 25° half angle cone are made at free-stream conditions corresponding to two CUBRC experiments (Runs 28 and 35). Results presented identify the sensitivity of the surface quantities (heating, pressure, and skin friction) to several physical model and numerical parameters. Also, information concerning the flow structure and comparison of surface results with the CUBRC experiments and other calculations is presented. Careful comparisons and analyses of computational and experimental results are essential in establishing confidence in both the data and the computational tools.

G2 DSMC CODE

The DSMC code used in the current study is the general 2D/axisymmetric code of Bird [12,13], called G2. The molecular collisions are simulated with the variable hard sphere (VHS) molecular model. Energy exchange between kinetic and internal modes is controlled by the Larsen-Borgnakke statistical model [14]. For the present study, the simulations are performed by using nonreacting gas models while considering energy exchange between translational, rotational, and vibrational modes. The model surface is assumed to have a specified constant temperature. Full thermal accommodation and diffuse reflection are assumed for the gas-surface interactions.

For most G2 simulations, the computational domain consists of an arbitrary number of regions. Each region is subdivided into cells in which the collision rate is set by the cell average properties. Also, the cells in selected regions can be subdivided into subcells to enhance the spatial resolution used to select collision partners and thereby minimize the loss of angular momentum. In general, the cell dimensions within a region are nonuniform in both directions, with geometric stretching being invoked. The macroscopic quantities are time-averaged results extracted from the individual cells. Since the computational regions are usually run with different time steps, it is essential that steady state conditions be established before generating the final time-averaged results. Steady state is assumed to occur when all molecules used in the simulation, the average molecules used in each region, and the surface quantities become essentially constant when sampled sequentially over significant time intervals. Most of the simulations made in the current study used a simple two-region domain, a small region upstream of the cone and one region above the cone, where the cells were not subdivided into additional subcells.

RESULTS AND DISCUSSION

Details of the model configuration that was used in the CUBRC tests are presented in Fig. 1. For this sharp double cone model, the first cone has a half angle of 25° and the second cone has a half angle of 55°. The projected length of the first cone on the x-axis is noted as L and has a value of 92.07 mm. A shortened version of the 25° sharp cone is considered in the current investigation, with the cone terminated at an x-location of 60 mm (x/L = 0.652). The shortened cone is sufficiently long to include all measurements made along the first cone (Figs. 2 and 3) that are upstream of any influence produced by the second cone. To maintain consistency with previously published results, the length L will be used as a nondimensionalizing quantity. Also, the characteristic length used to define the free-stream Reynolds number (Table 1) is L, even though the cone length used in the current study is only 65 percent of L.

Table 1 provides a summary of the specified free-stream and surface boundary conditions used for the two experimental test cases investigated. The experiments were performed in the Veridian Engineering 48-inch Hypersonic Shock Tunnel (HST). Note that the specified free-stream conditions are similar; yet, these differences were sufficient to produce a different extent of separation (Figs. 2 and 3) for the double cone experiments. The measured heating and pressure coefficient values are shown in Figs. 2 and 3 for Runs 28 and 35, respectively. Also included in Fig. 2 are the DSMC results obtained by Moss [8] with the G2 code. Two obvious discrepancies are evident between the calculated and measured results, the heating values upstream of the interaction region and the extent of separation. Subsequent calculations [11] obtained with the DAC (DSMC Analysis Code) code of LeBeau [15] have shown that the lack of agreement for the extent of separation is primarily a cell resolution issue [11]. However, the heating disagreement upstream of the interaction region is still present; that is, the DAC and G2 heating results are in excellent agreement upstream of the interaction region, but they are substantially higher than the experimental values.

The remaining discussion will focus on the calculations made for each of the two experimental test conditions. Results for Run 35 conditions are presented first and emphasize the effect of grid, comparisons with experiment [1], comparisons with the DSMC results of Wang and Boyd [10], and details concerning the flow structure. A similar, but more abbreviated presentation and discussion will follow for Run 28 conditions.

Results for Run 35 Conditions

Figures 4 through 18 present representative results from the current G2 simulation for Run 35 conditions. Information concerning the computational domain and Mach contours (1.0 and 11.2) is demonstrated in Fig. 4

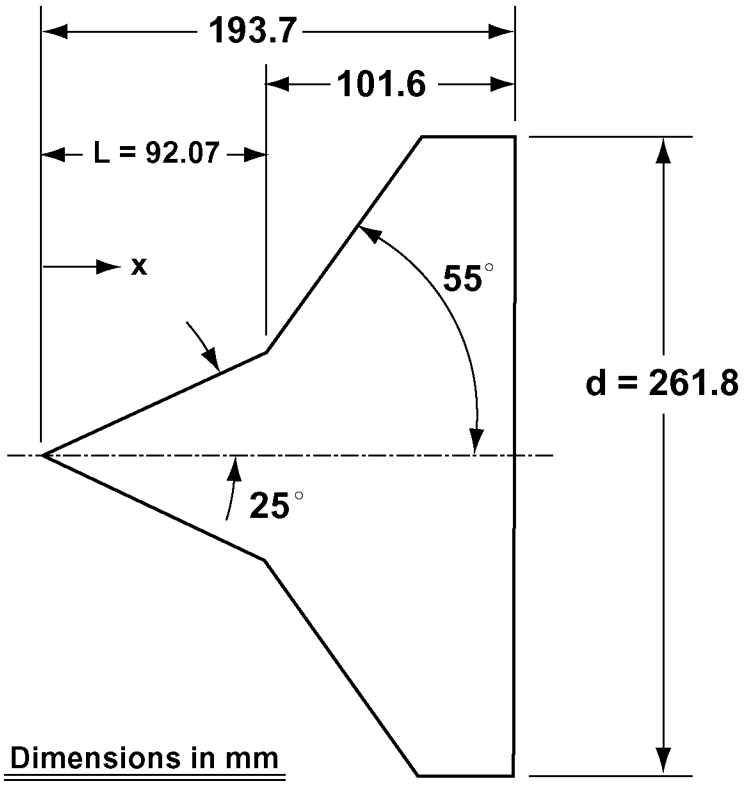

FIGURE 1. CUBRC sharp double cone model where x is measured from the vertex.

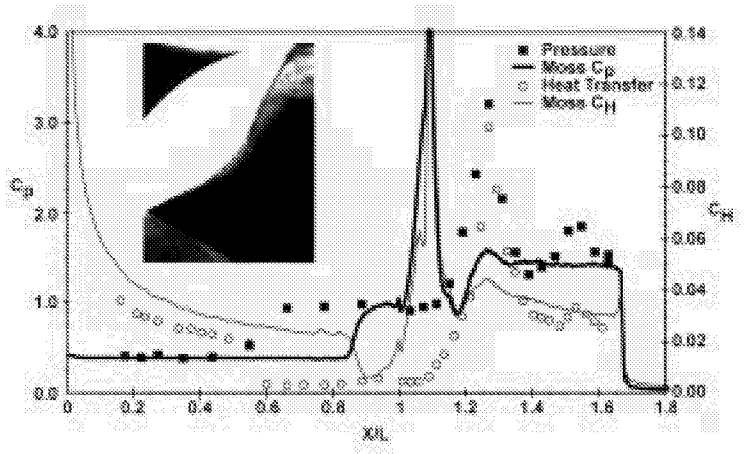

FIGURE 2. Calculated and measured surface coefficients (heating and pressure) for Run 28 (from Ref. [2]).

for the most resolved of the two grids considered. As is evident in Fig. 4, the subsonic flow region is very thin as the Mach 1 contour is extremely close to the cone surface. Also included in Fig. 4 is information concerning the computational domain, which consisted of two regions. Each region is subdivided into cells where the time step (Δt) and the number of real molecules each simulated molecule (FNUM) represents are constant within

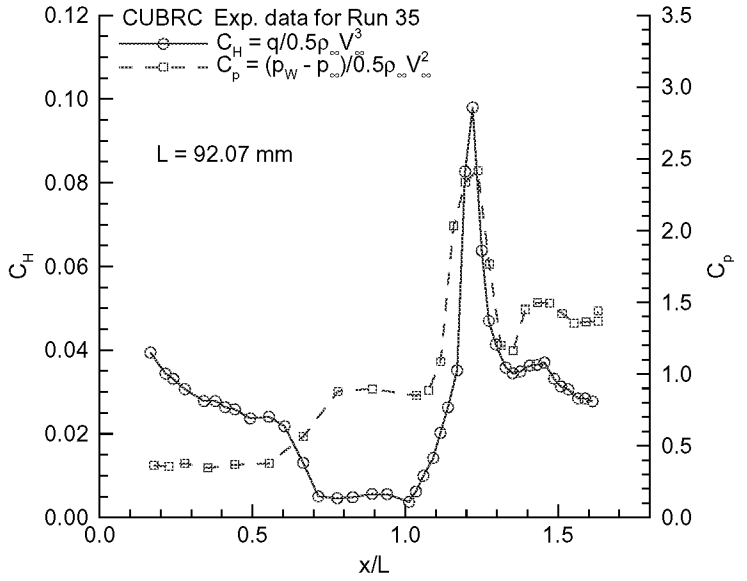

FIGURE 3. Measured surface heating and pressure coefficients for Run 35 (Ref. [1]).

TABLE 1. Free-Stream and Surface Conditions for Experiments Conducted in the 48-inch HST

Exp. Run No.	V_∞, m/s	$\rho_\infty \times 10^4$, kg/m^3	$n_\infty \times 10^{-22}$, m^{-3}	T_∞, K	p_∞, N/m^2	Gas	M_∞	$Re_{\infty,L}$	T_W, K
28	2 664.0	6.546	1.407	185.6	36.05	Nitrogen	9.59	13 253	293.3
35	2 712.2	5.520	1.186	138.9	22.75	Nitrogen	11.29	14 142	296.1

a region. Time step information for each region and the region 1 time interval, for which the time-averaged results were obtained, are included in Fig. 4. Steady state was assumed to occur when the total molecules used in the simulation, the average molecules per cell in each region, and the values of the surface quantities became essentially constant when sampled over some significant time interval. The first two criteria are demonstrated in Fig. 5 for the fine grid simulation. With a region 1 time step of 4 nanoseconds (ns), 130 000 time steps were used in this simulation.

With the specified quantities for grid and time step information, the time step was less than the time required to transverse a cell. Also, the cell dimensions were such that the dimension in the radial direction adjacent to the surface was less than 0.6 times the local mean free path, and its maximum value within the computational domain was 1.8. With the use of high aspect ratio cells, the cell dimensions in the x-direction had much larger values in relation to the local mean free path, ranging from a minimum of 3 to a maximum of 38. The population of simulated molecules per cell ranged from a minimum of 3 to a maximum of 75. Each regional average number of molecules per cell is presented in Fig. 5.

Figure 6 presents a comparison of surface distributions for heating rate, pressure, and friction that is computed with the grid previously described and one with a coarser gird, having only 40 percent of the cells that the finer grid has. The cell distribution over the cone for the coarser grid was 100 x 160 instead of 200 x 200. As shown in Fig. 6, the surface distributions are in excellent agreement for the two solutions, with the only differences occurring near the tip of the model (obvious with an enlarged view) where the simulation becomes more accurate as the axial step size is reduced.

Comparisons of the present results with the CUBRC measurements [1] and the DSMC calculations made with the MONACO [10] code are shown in Figs. 7 through 10. The current predictions (Fig. 7) for heating

rates are noticeably higher than the experimental values; in fact, they are 25 percent higher, as shown in Fig. 8, where the experimental data have been modified by a constant factor of 1.25. These differences between the G2 calculations are consistent with what has been observed [11] for other CUBRC experiments involving the heating-rate measurements along the hollow cylinder of a hollow cylinder-flare model (factors of 1.17 for Run 11 and 1.25 for Run 9).

As shown in Fig. 7, the MONACO predictions for heating rate are in excellent agreement with the measured values. Based on these findings, several basic questions arise. Should either of the two calculations agree with the measurements based on the accuracy with which the measurements have been made and the accuracy with which the free-stream conditions/test environment have been specified? Why the substantial difference between the two DSMC results for the same specified free-stream conditions? Currently, answers to these questions are not apparent. However, some additional comparisons of the computational results are presented in Fig. 9, which shows that there are noticeable differences in all surface predicted quantities. On a percentage basis, the differences in predicted heating and friction are comparable; the current results are about 25 percent higher than the MONACO values. A more detailed comparison of the pressure is shown in Fig. 10, which also includes the experimental data. The experimental pressure data are not that definitive since they exhibit considerable scatter and the magnitude of the data is lower than that given by the inviscid cone value of 0.38 (Ref. [16], Fig. 6). Since the flow along the cone is in the strong hypersonic interaction regime based on standard viscous interaction parameters (see Ref. [8]), one would expect that the inherent displacement effects of the viscous flow would produce pressure values in excess of the inviscid compressible flow values; yet, both the experimental and MONACO pressure coefficient values are less than 0.38 for the region where the measurements were made.

There are differences in the physical models and the computational cell size and arrangement used in the G2 and MONACO calculations. For example, the number of cells used in the MONACO simulation was an order of magnitude greater than the finest grid used in the G2 simulation (Fig. 7). However, it is not obvious that these differences can account for the large discrepancies observed in surface heating and skin friction.

Figures 11 and 12 provide information describing the flow structure for the short cone. Contours for nondimensional density and overall kinetic temperature are included. Additional information concerning the flow structure and rarefaction effects are evident in the radial profiles presented in Figs. 13 through 18. The current flow is characterized as a merged layer near the model vertex to one with a distinct shock and inviscid/boundary layer regions downstream. Also, thermal nonequilibrium is evident in the shock crossings when the overall kinetic temperature profiles (Fig. 15) are compared with the corresponding translational temperature profiles (Fig. 16). A more specific example of the thermal nonequilibrium effect is demonstrated in Fig. 18 where three radial temperature profiles (overall, translational, and rotational) are included for $x/L = 0.3$. Except for the shock crossing, the three temperature profiles are in close agreement at this cone location. Also, an appreciable temperature jump (Fig. 15) and velocity slip (Fig. 17) are predicted and are in qualitative agreement with the MONACO results described in Ref. [10].

Results for Run 28 Conditions

An abbreviated summary of the calculations for CUBRC Run 28 conditions are included to make the point that the differences observed in the experimental and computational results are of similar magnitude for similar flow conditions (Table 1), not an isolated occurrence. The experimental results [1] for heating and pressure coefficients are presented in Fig. 19, where spline curves have been used to join the individual data points. The current focus is on the results, particularly the heating results, along the sharp cone, upstream of any influence of the second cone; that is, for x/L values less than about 0.55.

The current calculations were made by using the G2 code for the same length cone as for the Run 35 simulations. The grid had a total of 16 400 cells with 100 x 160 cells in region 1 (see Fig. 4): that is, the coarser of the two grids was used for the Run 35 simulations. The heating rate results obtained with the short cone are in excellent agreement with the full body solution shown in Fig. 2. Comparisons of the current results with the Navier Stokes (NS) solutions of Gnoffo [4] (the code LAURA with prefect gas and no slip boundary conditions), and the CUBRC data are displayed in Figs. 20 through 23. As shown in Fig. 20, the current DSMC results for the sharp cone and the NS results for the double cone are in close agreement, particularly in the region where measurements have been made upstream of the interaction region. The good agreement between the two codes may be fortuitous since velocity slip and temperature jump are evident in the DSMC results (not shown, but similar to that for Run 35) and the NS calculation was made with the no slip and

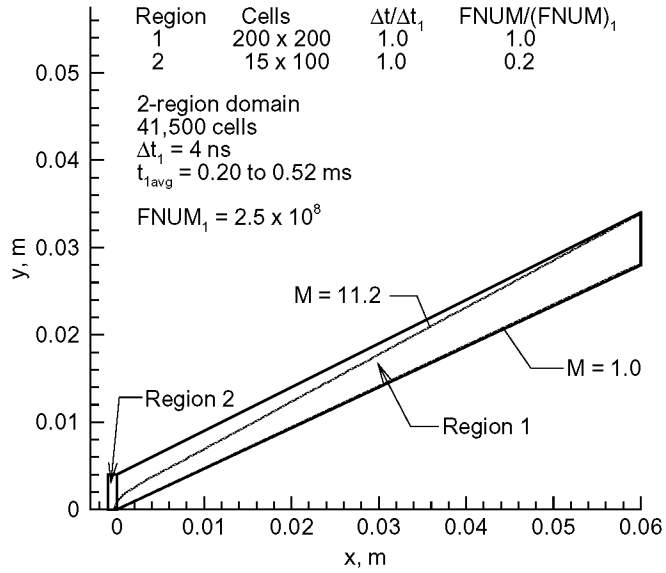

FIGURE 4. Simulation parameters and resulting flow structure (Mach contours) for Run 35 conditions.

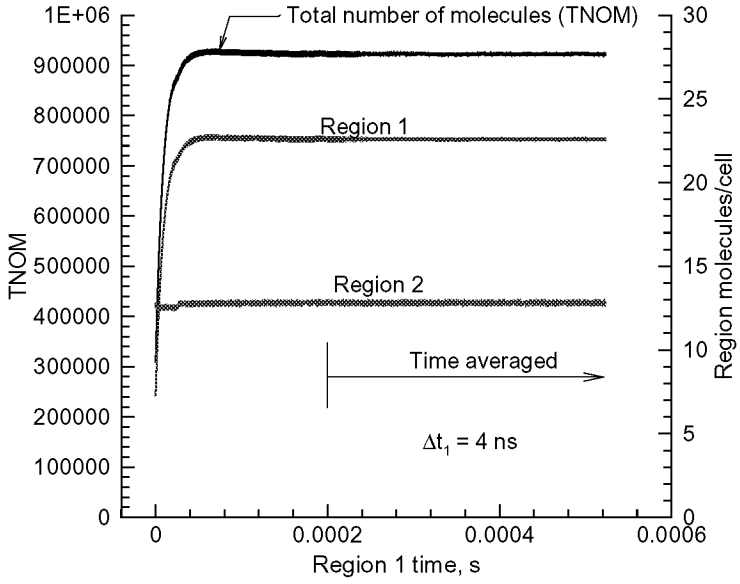

FIGURE 5. Simulation history with fine grid for Run 35 conditions.

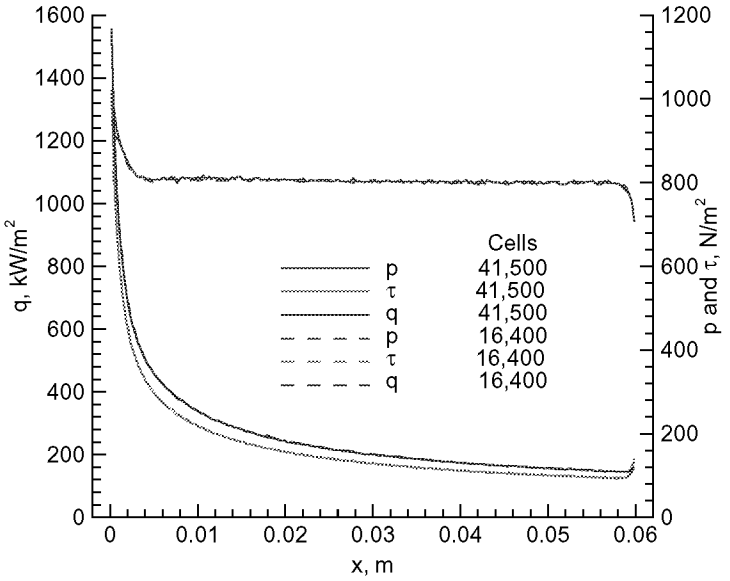

FIGURE 6. Effect of grid on calculated surface heating rate, pressure, and skin friction distributions.

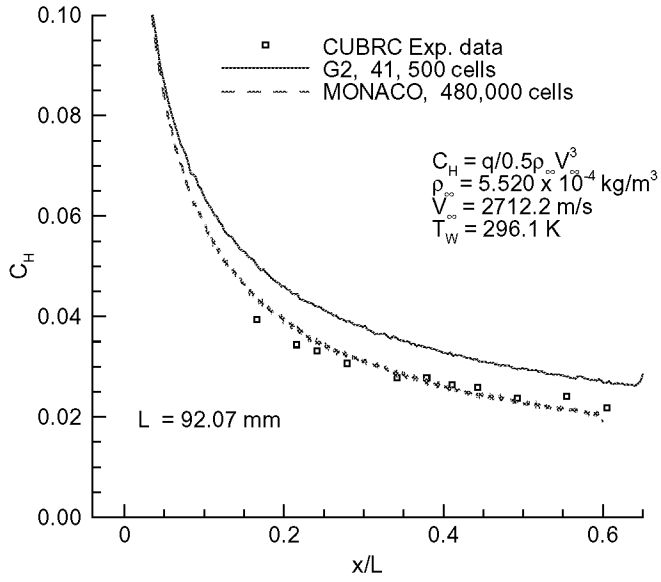

FIGURE 7. Comparison of heating distributions: present G2 results, MONACO [10], and experiment [1].

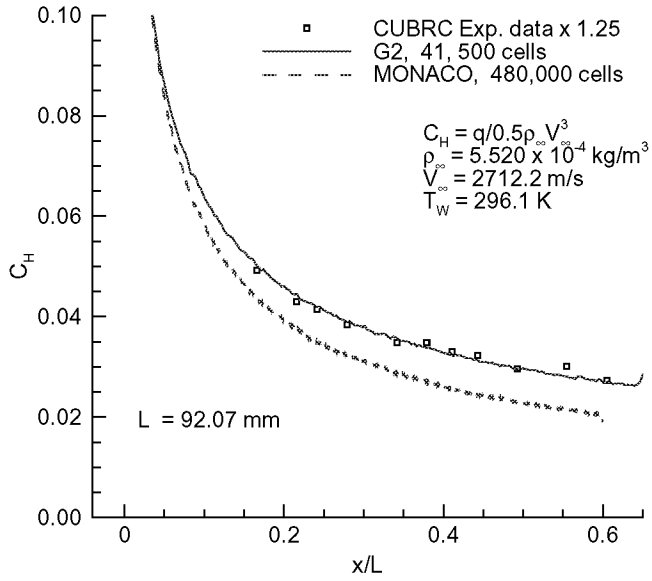

FIGURE 8. Comparison of heating distributions: present G2 results, MONACO [10], and modified CUBRC data.

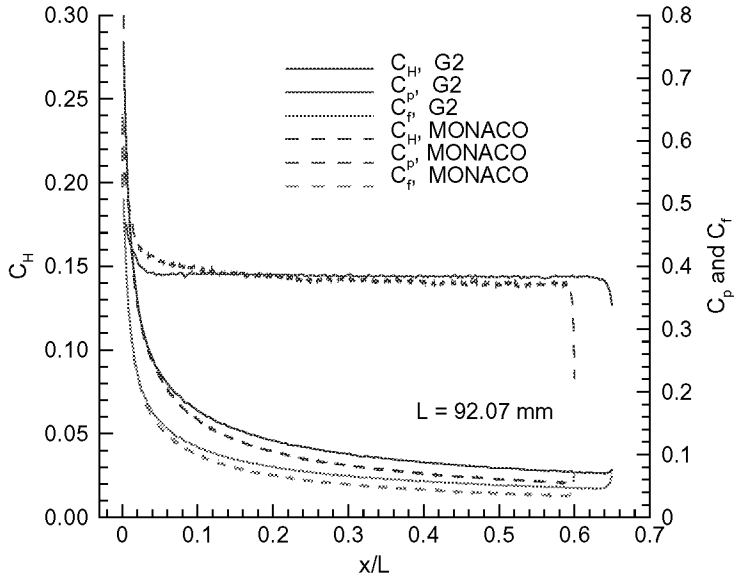

FIGURE 9. Comparison of G2 and MONACO [10] surface distributions for Run 35 conditions.

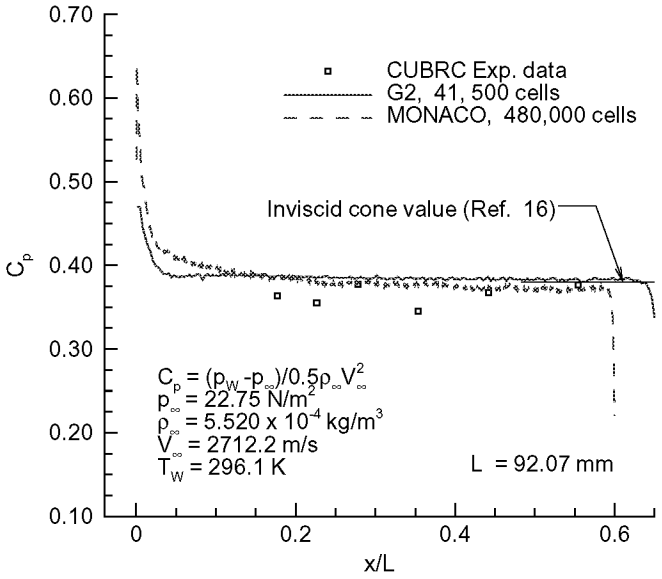

FIGURE 10. Comparison of pressure distributions: present G2 results, MONACO [10], and CUBRC data [1].

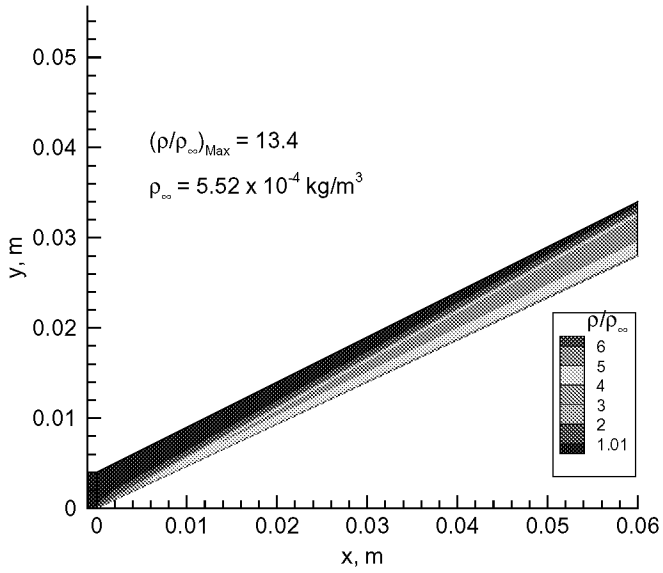

FIGURE 11. Density contours for Run 35 conditions.

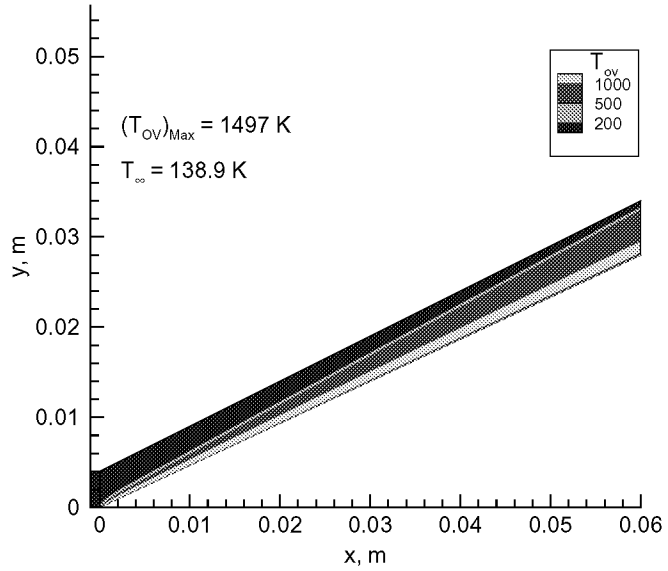

FIGURE 12. Overall kinetic temperature contours for Run 35 conditions.

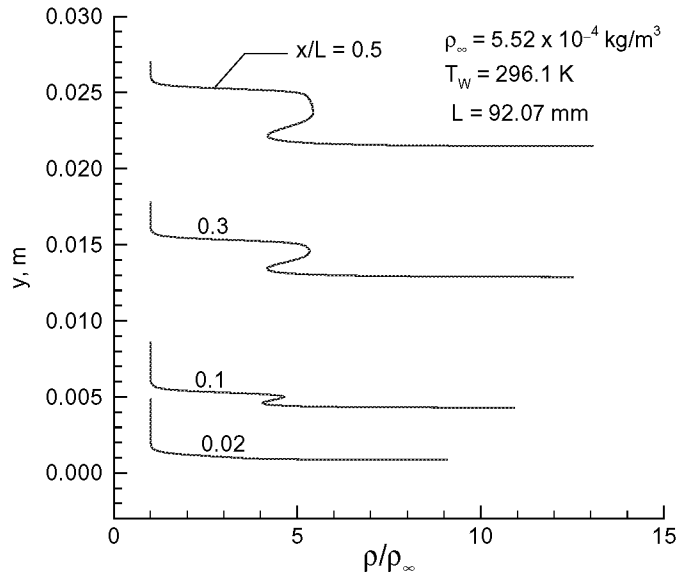

FIGURE 13. Radial density profiles at four x-locations along cone for Run 35 conditions.

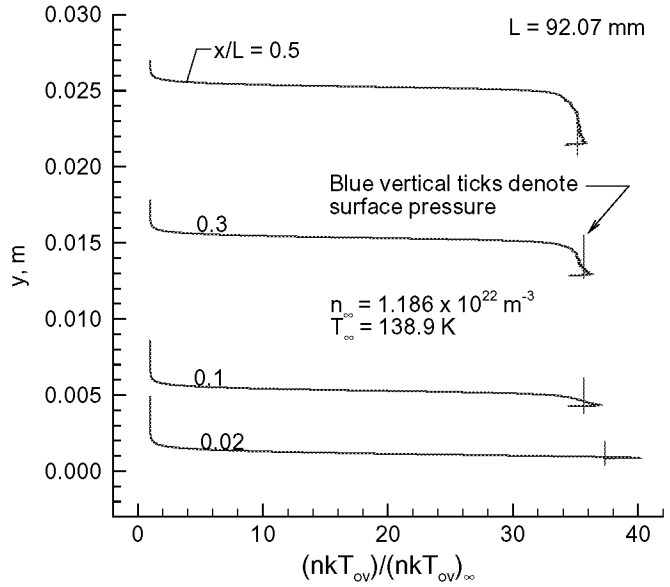

FIGURE 14. Radial static pressure profiles at four x-locations along cone for Run 35 conditions.

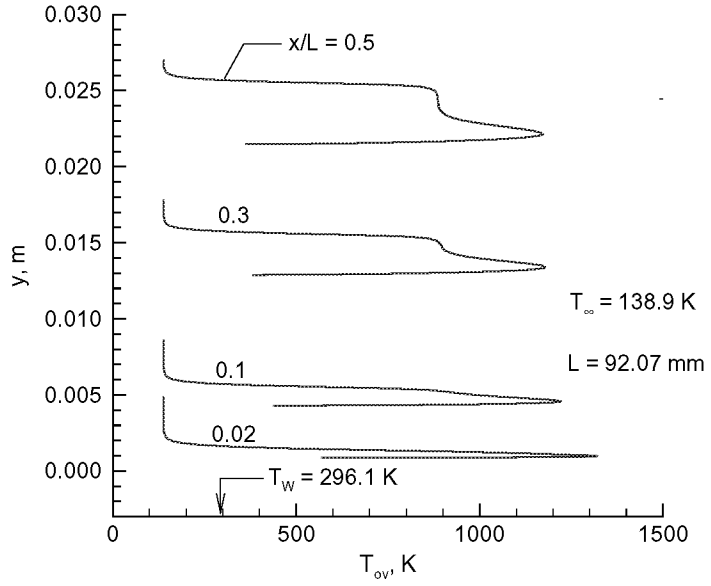

FIGURE 15. Radial overall kinetic temperature profiles at four x-locations along cone for Run 35 conditions.

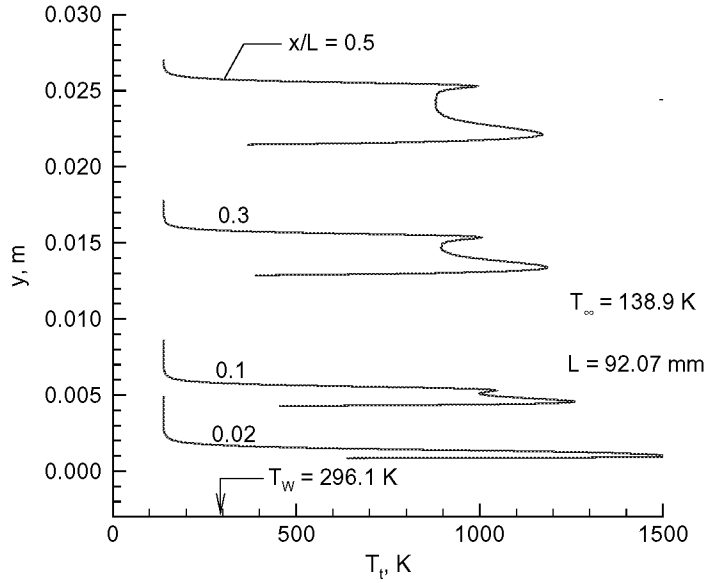

FIGURE 16. Radial translational temperature profiles at four x-locations along cone for Run 35 conditions.

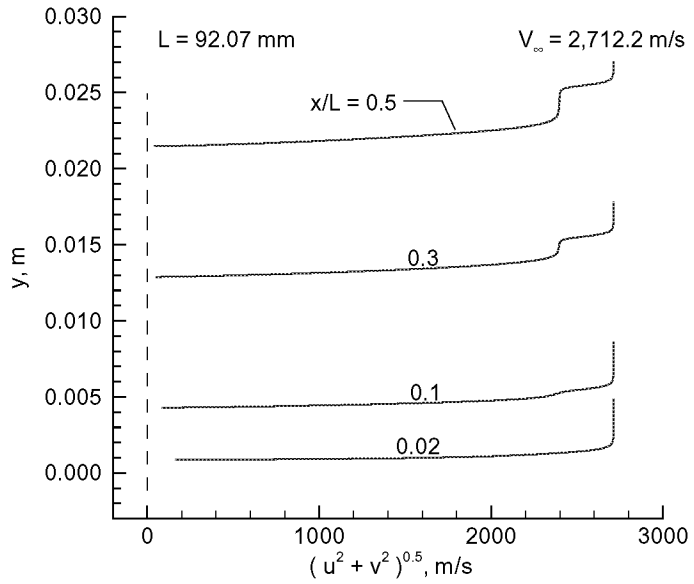

FIGURE 17. Radial speed profiles at four x-locations along cone for Run 35 conditions.

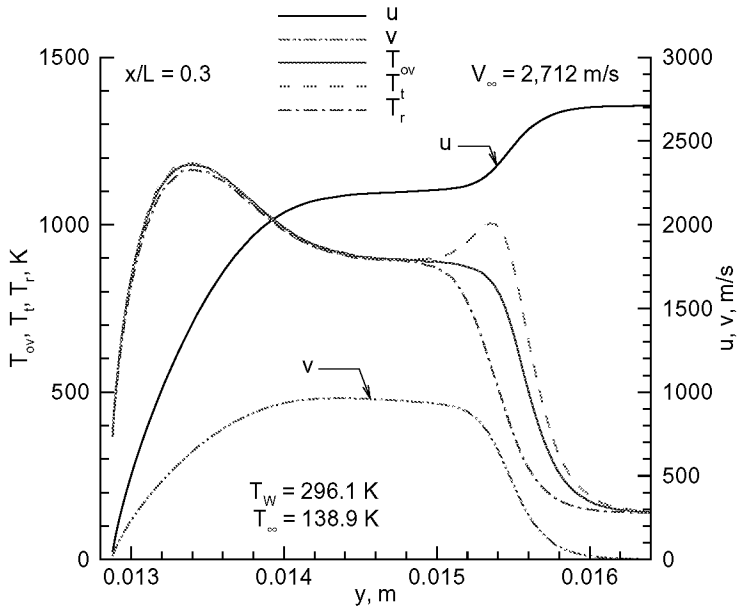

FIGURE 18. Temperature and velocity radial profiles at x/L = 0.3 for Run 35 conditions.

no temperature jump surface boundary assumption. The calculated values for heating are high in relation to the measured values (Fig. 21), about 33 percent higher, as demonstrated in Fig 22, where the experimental data have been adjusted by a factor of 1.33. The calculated data for the pressure coefficients (Fig. 23) are, in general, lower than the measured values, opposite the trend observed for Run 35 conditions. For the current case, the experimental and computed values are equal to or greater than the inviscid cone value of 0.38.

The large differences observed in measured and calculated heating values have been observed [2] in other CFD calculations. Of the five computational solutions presented for this test case (three NS and two DSMC), all solutions are in close agreement with the present results, with the exception of the DSMC results of Boyd and Wang obtained with the MONACO code [7], which are in good agreement with the experimental results. An obvious difference in the current calculations and those of Boyd and Wang is the assumption concerning the surface boundary conditions in which they assumed the gas-surface interactions to be 85 percent diffuse and 15 percent specular, rather than the current assumption of fully diffuse. However, these two boundary conditions have been shown to give the same results for heating, using either the G2 [11] or the MONACO [10] codes.

A potential explanation for the discrepancy between the current calculated and the measured heating rates is discussed in Ref. [6], where it is shown that the sensitivity of the surface heating and pressure values to uncertainties in the vibrational energy state at the test section far outweigh the uncertainties in the surface measurements. For the limiting case in which the vibrational temperature in the free stream was assumed to be frozen at the stagnation temperature (frozen nozzle expansion), but where the total energy level was held constant at the baseline energy, the surface heating rates predicted with a DSMC code were 25 percent lower than those predicted for the specified nominal free-stream conditions, conditions inferred by assuming thermal equilibrium during the nozzle expansion. These differences are similar to the differences observed in the current study; that is, the experimental heating-rate values are 20 and 25 percent lower than the calculated values for Runs 35 and 28, respectively. However, the vibrational freezing is unlikely to be either instantaneous or at a total temperature value. Consequently, an investigation is warranted to identify the impact of thermal nonequilibrium on the test environment and on the calculated surface heating rates.

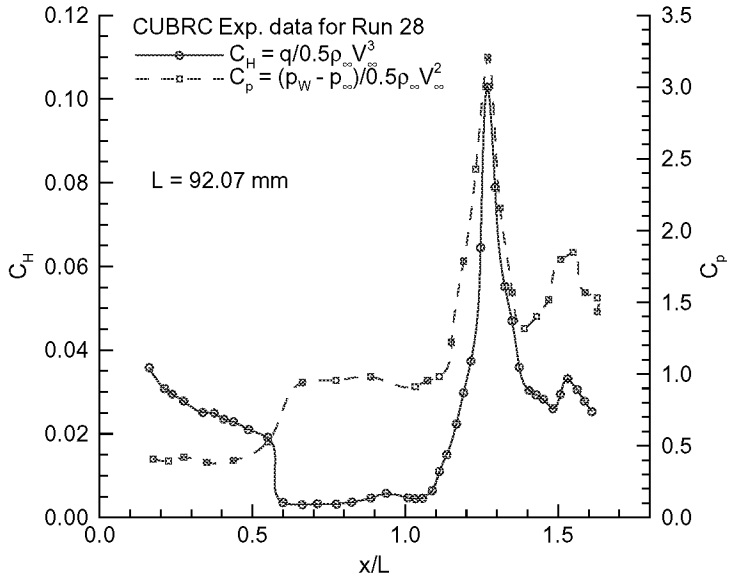

FIGURE 19. Measured surface heating and pressure coefficients for Run 28 (Ref.1).

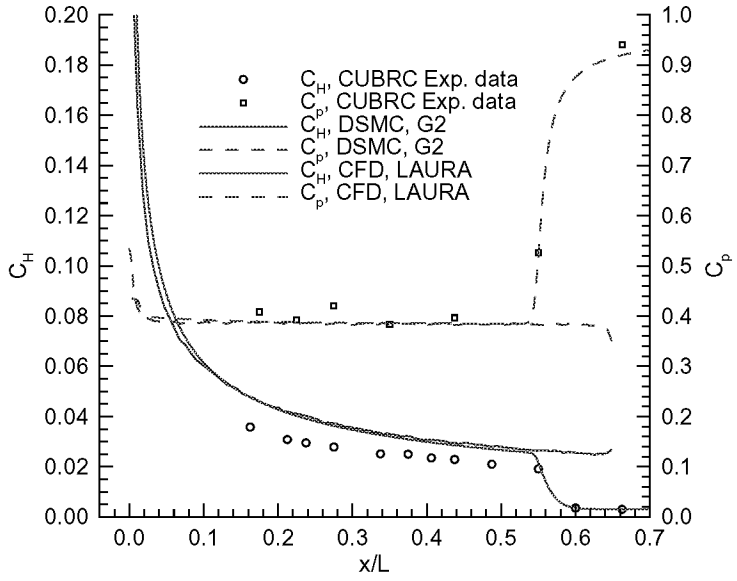

FIGURE 20. Comparison of surface heating and pressure coefficients for Run 28: present G2 results, LAURA [4], and CUBRC data.

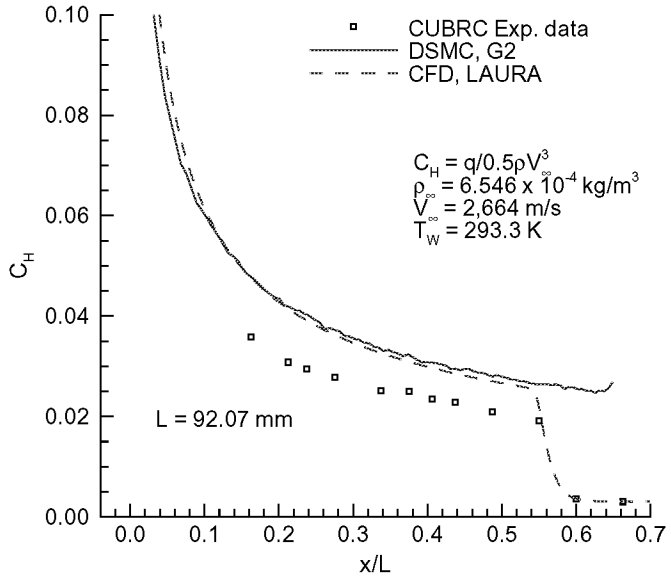

FIGURE 21. Comparison of surface heating for Run 28: present G2 results, LAURA [4], and CUBRC data.

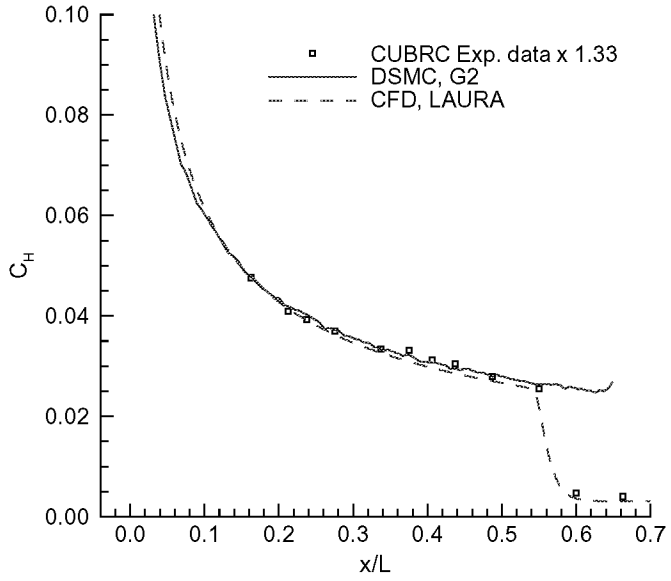

FIGURE 22. Comparison of surface heating for Run 28: present G2 results, LAURA [4], and modified CUBRC data.

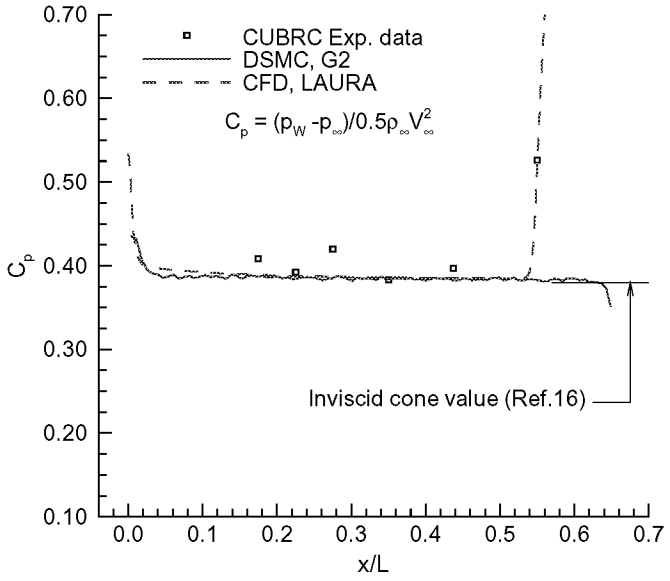

FIGURE 23. Comparison of surface pressure for Run 28: present G2 results, LAURA [4], and CUBRC data.

CONCLUDING REMARKS

Results of a computational study are presented for hypersonic nitrogen flows about a sharp cone model having a half angle of 25° degrees. The free-stream conditions are those specified for two experiments conducted by CUBRC while using the Veridian 48-in Hypersonic Shock Tunnel. Computations are made with the DSMC method by using the G2 code of Bird. The focus of the current study is to highlight the significant differences that have been observed between measured and calculated results for heating on the sharp cone portion of the CUBRC experiments when using double cone models. The current results show that the predicted heating rates are 25 and 33 percent higher than the measured values for the two cases examined, Runs 35 and 28, respectively. Comparisons with other published computations show that the current results are in close agreement with other CFD results that have been obtained with a no slip and no temperature jump boundary condition. The only solutions that have been presented that agree well with the CUBRC results for the sharp cone are the DSMC solutions obtained with the MONACO code.

A key issue still outstanding is the problem of identifying the source of the significant differences observed in predicted surface quantities. With the current test cases showing evidence of surface slip and temperature jump effects, the first order of business should be to resolve the differences among the DSMC codes. If the source of the differences can be resolved, differences between computation and experiment may or may not remain an issue. (**Note** that a mistake was recently found [17] in the implementation of the variable soft sphere collision model used in the MONACO simulations. When the MONACO simulation was made with a variable hard shpere model, same as used in the current G2 simulations, the heating-rate predictions were similar to the current G2 results; that is, high in relation to the experimental measurements.)

For the current experimental test cases, the measured heating rates are 20 and 25 percent low with respect to the calculated G2 results for Runs 35 and 28, respectively. The computational study of Roy et al. [6] has shown that thermal nonequilibrium effects within the test section can produce this order of magnitude reduction in predicted heating rates, provided the vibrational temperature is assumed frozen at the stagnation temperature during the nozzle expansion. Additional studies are required to identify the effects of vibrational freezing (thermal nonequilibrium) on both the test environment and on the calculated surface results, particularly the effect on surface heating.

Beyond identifying the differences among the DSMC codes and the thermal nonequilibrium effects on the test environment, there is a need for a thorough reconciliation of the calibration and test measurements with calculations for the current test conditions. Specifically, what are the rake survey results at the test location and what are the results for the pitot tube and hemispherical heat transfer probe measurements made off the centerline during the actual tests (Runs 28 and 35)? Establishing a clearer understanding of the flow nonuniformity and the consistency of the measured and calculated heating rates for both the test model and the off-centerline probes is an essential requirement of the ongoing reconciliation activities.

ACKNOWLEDGMENTS

The author acknowledges the assistance of Michael S. Holden and Timothy P. Wadhams of CUBRC for providing information regarding the model configuration, flow conditions, and experimental data. Also, the assistance of several individuals is very much appreciated for providing computational results: Iain D. Boyd and Wen-Lan Wang of the University of Michigan (DSMC results from the MONACO code), and Peter A. Gnoffo of the NASA Langley Research Center (Navier Stokes results from the LAURA code).

REFERENCES

1. Holden, M. S., and Wadhams, T. P., "Code Validation Study of Laminar Shock/Boundary Layer and Shock/Shock Interactions in Hypersonic Flow Part A: Experimental Measurements," AIAA Paper 2001-1031, Jan. 2001.
2. Harvey, J. K., Holden, M. S., and Wadhams, T. P., "Code Validation Study of Laminar Shock/Boundary Layer and Shock/Shock Interactions in Hypersonic Flow Part B: Experimental Measurements," AIAA Paper 2001-1031, Jan. 2001.
3. Candler, G. V., Nompelis, I., and Druguet, M.-C., "Navier-Stokes Predictions of Hypersonic Double-Cone and Cylinder-Flare Flow Fields," AIAA Paper 2001-1024, Jan. 2001.
4. Gnoffo, P. A., "CFD Validation Studies for Hypersonic Flow Prediction," AIAA Paper 2001-1025, Jan. 2001.
5. Kato, H., and Tannehill, J. C., "Computation of Hypersonic Laminar Separated Flows Using an Iterated PNS Algorithm," AIAA Paper 2001-1028, Jan. 2001.
6. Roy, C. J., Bartel, T. J., Gallis, M. A., and Payne, J. L., "DSMC and Navier-Stokes Predications for Hypersonic Laminar Interacting Flows," AIAA Paper 2001-1030, Jan. 2001.
7. Boyd, I. D., and Wang, W.-L., "Monte Carlo Computations of Hypersonic Interacting Flows," AIAA Paper 2001-1029, Jan. 2001.
8. Moss, J. N., "DSMC Computations for Regions of Shock/Shock and Shock/Boundary Layer Interaction," AIAA Paper 2001-1027, Jan. 2001.
9. Markelov, G. N., Walpot, L., and Ivanov, M. S., "Numerical Simulation of Laminar Hypersonic Separation Using Continuum and Kinetic Approaches," AIAA Paper 2001-2901, June 2001.
10. Wang, W.-L., Boyd, I. D., Candler, G. V., and Nompelis, I., "Particle and Continuum Computations of Hypersonic Flow Over Sharp and Blunted Cones," AIAA Paper 2001-2900, June. 2001.
11. Moss, J. N., and LeBeau, G. J., "Hypersonic Separated Flow Simulations Using DSMC," AIAA Paper 2002-0214, Jan. 2002.
12. Bird, G. A., "The G2/A3 Program System Users Manual," Version 1.8, March 1992.
13. Bird, G., *Molecular Gas Dynamics and the Direct Simulation of Gas Flows*, Oxford: Clarendon Press, 1994.
14. Borgnakke, C. and Larsen, P. S., "Statistical Collision Model for Monte Carlo Simulation of Polyatomic Gas Mixture," *Journal of Computational Physics*, Vol. 18, No. 4, 1975, pp. 405-420.
15. LeBeau, G. J.,"A Parallel Implementation of the Direct Simulation Monte Carlo Method," *Computer Methods in Applied Mechanics and Engineering*, Vol. 174, 1999, pp. 319-337.
16. Ames Research Staff; *Equations, Tables, and Charts for Compressible Flow.* NACA Report 1135, 1953.
17. Boyd, I., private communication, September 18, 2001.

REPORT DOCUMENTATION PAGE

Form Approved
OMB No. 0704-0188

1. AGENCY USE ONLY (*Leave blank*)	2. REPORT DATE	3. REPORT TYPE AND DATES COVERED
	December 2001	Technical Memorandum

4. TITLE AND SUBTITLE
Hypersonic Flows About a 25° Sharp Cone

5. FUNDING NUMBERS
WU 706-85-40-02

6. AUTHOR(S)
James N. Moss

7. PERFORMING ORGANIZATION NAME(S) AND ADDRESS(ES)
NASA Langley Research Center
Hampton, VA 23681-2199

8. PERFORMING ORGANIZATION REPORT NUMBER
L-18122

9. SPONSORING/MONITORING AGENCY NAME(S) AND ADDRESS(ES)
National Aeronautics and Space Administration
Washington, DC 20546-0001

10. SPONSORING/MONITORING AGENCY REPORT NUMBER
NASA/TM-2001-211253

11. SUPPLEMENTARY NOTES

12a. DISTRIBUTION/AVAILABILITY STATEMENT
Unclassified-Unlimited
Subject Category 34 Distribution: Standard
Availability: NASA CASI (301) 621-0390

12b. DISTRIBUTION CODE

13. ABSTRACT (*Maximum 200 words*)
This paper presents the results of a numerical study that examines the surface heating discrepancies observed between computed and measured values along a sharp cone. With Mach numbers of an order of 10 and the free-stream length Reynolds number of an order of 10 000, the present computations have been made with the direct simulation Monte Carlo (DSMC) method by using the G2 code of Bird. The flow conditions are those specified for two experiments conducted in the Veridian 48-inch Hypersonic Shock Tunnel. Axisymmetric simulations are made since the test model was assumed to be at zero incidence. Details of the current calculations are presented, along with comparisons between the experimental data, for surface heating and pressure distributions. Results of the comparisons show major differences in measured and calculated results for heating distributions, with differences in excess of 25 percent for the two cases examined.

14. SUBJECT TERMS
Hypersonic, DSMC computations, experimental heating-rate measurements, cone flow

15. NUMBER OF PAGES
22

16. PRICE CODE

17. SECURITY CLASSIFICATION OF REPORT	18. SECURITY CLASSIFICATION OF THIS PAGE	19. SECURITY CLASSIFICATION OF ABSTRACT	20. LIMITATION OF ABSTRACT
Unclassified	Unclassified	Unclassified	UL